A MIMO Antenna Utilizing Modified Apollonian Fractal for Sub-6 5G Wireless Applications

Abubeker A. Yussuf*, Selçuk Paker**

* Corresponding Author, Dr., Department of Electronic and Communication Engineering, Istanbul Technical University, Maslak, 34469, Istanbul, Türkiye. ORCID: 0009-0001-1403-1049

‡* Prof. Dr., Department of Electrical and Electronics Engineering, Istanbul Nişantaşı University Sarıyer, 34375, Istanbul, Türkiye. ORCID: 0000-0002-1769-1835

(yussuf@itu.edu.tr, abubeker2008@gmail.com, selcuk.paker@nisantasi.edu.tr)

Received: 03.09.2024 Accepted: 30.06.2025

Abstract- In this paper, a quad-element multiple-input multiple-output (MIMO) antenna is designed using a modified Apollonian fractal shape for 5G Wireless communication. The proposed antenna comprises four radiating Apollonian fractal elements placed at optimal positions, along with a bottom layer incorporating a segmented ground plane. Each radiating element is composed of a microstrip feed with a quarter-wave transformer to improve impedance matching. The proposed Apollonian fractal-shaped MIMO antenna operates over the frequency range of 3.3–3.8 GHz, achieving an impedance bandwidth where S11 is less than -10 dB and mutual coupling below -20 dB. The envelope correlation coefficient (ECC) remains below 0.05, ensuring excellent diversity performance. Furthermore, the performance parameters of the Apollonian fractal- shaped MIMO antenna are evaluated based on S-parameters, such as the envelope correlation coefficient and channel capacity. Experimental measurements show that the ECC is lower than 0.05, while the channel capacity loss is below 0.6, reflecting reasonable agreement with the simulation results.

Keywords: Apollonian fractal, quarter-wave transformer, MIMO, S-parameters, ECC, channel capacity

1. Introduction

Fifth-generation (5G) is the latest evolution in mobile and wireless communication technology, characterized by high speed, low latency, and substantial data rates [1]. The 5G spectrum is categorized into low- to mid-band frequencies below 6 GHz, and high-band spectrum utilizing millimeter waves (mm- Wave) [2]. Currently, 5G technology is being employed across specific spectrum bands, such as the mid-band (NR Band 78: 3.3–3.8 GHz and NR Band 79: 4.4–5.0 GHz) and the high-band (NR Band 258: 24.25–27.5 GHz and NR Band 260: 37–40 GHz). The mid-band spectrum is required to have at least 100 MHz of bandwidth to support the data rate and technical requirements of 5G [3]. The rapid development of wireless devices and networks continues to expand with the application of emerging technologies such as MIMO antennas. MIMO antennas are particularly attractive for deployment in portable wireless communication devices for 5G applications, as they provide high data rates and improved channel capacity [4].

Over the past few years, various studies have proposed the design of MIMO antennas based on fractal structures. Fractal geometry enables antenna miniaturization and broad bandwidth within limited space due to its inherent properties, such as self-repeating patterns and space-filling characteristics. For instance, Gurjar et al. [5] presented a dual-radiating element MIMO antenna featuring an 8-shaped self-affine fractal structure with a T-formed extension on the ground plane. This antenna achieved isolation of approximately 15 dB across a bandwidth ranging from 3.18

to 11.5 GHz. Bhattacharya et al. [6] proposed a twin monopole slotted antenna using a Koch snowflake shape, where the minimum isolation level exceeded 22 dB within a bandwidth of 3.0 - 11.1 GHz. Das et al. [7] introduced a hexagonal wide- slot antenna utilizing fractal geometry, achieving isolation greater than 18 dB across a bandwidth of 2.8811 GHz. Tripathi et al. [8] proposed an antenna design involving outer edges of two octagonal geometries using Koch fractal geometry, with an operating band spanning 3.18 to 11.5 GHz. From the above review, it is evident that many types of MIMO antennas have been designed utilizing several fractal geometries, such as the Sierpinski triangle and Koch snowflake. However, in this study, a new modified fractal-shaped MIMO antenna is designed using an Apollonian structure.

In this study, a four-radiating element antenna based on Apollonian geometry [9] is proposed for MIMO applications. The radiating elements are positioned orthogonally to exploit diversity in the proposed MIMO antenna. Additionally, the radiators are supplied by a microstrip line with a quarter-wave transformer for improved impedance matching. The Apollonian-shaped MIMO antenna offers a compact size with minimal inter-element mutual coupling and a low envelope correlation coefficient. This antenna, simulated using the commercial software, was fabricated and measured to verify its design. Its compact nature and performance make it ideal for integration into 5G mobile communication devices.

2. An Apollonian Fractal Configuration

A novel monopole antenna design, featuring an Apollonian fractal, is shown in Fig. 1. The figure shows the antenna's two-layer configuration, including a front layer with the Apollonian fractal and a back layer that functions as a ground plane. Furthermore, the figure includes a description of the iterative process used to generate the Apollonian fractal, as well as a magnified view of the top layer. A 50-ohm microstrip line is connected to the antenna, using a quarter-wave transformer for optimal impedance matching. The proposed design was aimed to resonate at n78 and utilized a circular patch, as suggested by Balanis [10]. The antenna was constructed on a PCB substrate featuring a 1.6 mm thickness, and a permittivity of 4.3. The overall dimensions of the antenna were 40 x 40 mm². Table 1 provides the optimized parameters used in the design of the Apollonian fractal monopole antenna. The Apollonian fractal structure was chosen for its unique properties, including self-similarity and space-filling characteristics, which facilitate antenna miniaturization and enhance performance in compact designs.

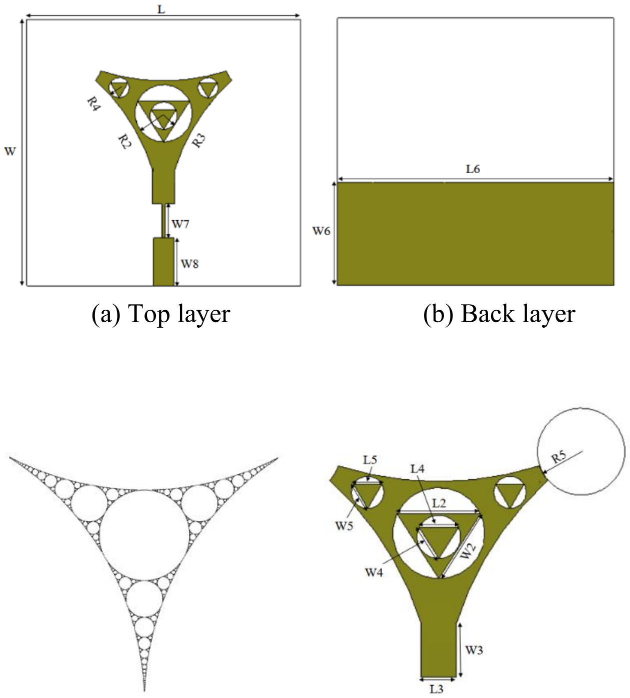

(a) Top layer (b) Back layer

(c) Apollony Fractal (d) Magnified top layer

Fig. 1. Geometry of a modified Apollony fractal antenna.

The hypothesis is that the fractal structure will improve impedance matching, reduce mutual coupling, and enhance radiation efficiency, making it suitable for MIMO applications in sub-6 GHz 5G bands.

Table 1. Optimized parameters of the Apollony fractal antenna.

P	Dim (mm)	P	Dim (mm)	P	Dim (mm)
L	40	L2	7.6	L3	3.2
W	40	W2	7.05	W3	4.9
L4	3.6	L5	2.6	L6	40
W4	3.37	W5	2.6	W6	17
R2	4.2	R3	2	R4	15
W7	5	W8	7	R5	2.84

P- Parameter Dim- Dimension

3. Design Evaluation

A four-phase design evaluation of an Apollonian fractal monopole antenna, used to verify the design, is presented in Fig. 2. Initially, the Apollonian structure was constructed by creating three circles with an equal radius of 30 mm, mutually tangent to each other, as shown in Fig. 1. The solid Apollonian structure, formed by the triangular region among the three mutually tangent circles, is depicted in Phase 1 with a microstrip feed. In Phase 2, the Apollonian fractal antenna was matched to the 50 Ω feed line using a quarter-wavelength transmission line, as illustrated in Fig. 2. In Phase 3, circles with radii of 4.2 mm and 1.5 mm were slotted at the center and two corners of the solid Apollonian fractal structure.

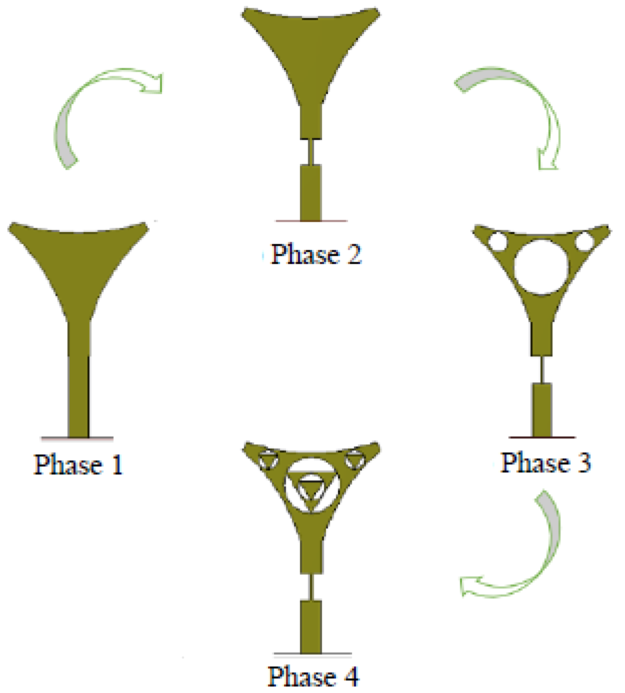

Fig. 2. Design evolution of the Apollony fractal antenna.

Finally, in Phase 4, the Apollonian fractal structure evolves into a self-replicating network of circular elements that integrate parasitic elements to enhance bandwidth, making it suitable for 5G NR Band 78. The evolution of the antenna design across four phases is illustrated by the simulated return loss presented in Fig. 3. Initially, the Phase 1 design resonated at 2.5 GHz, which shifted to 4 GHz in Phase 2 following the introduction of a quarter-wavelength transmission line; this modification primarily improved impedance matching and significantly enhanced the S_{11} parameter. Subsequent refinements in Phases 3 focused on further shifting the resonant frequency, with Phase 4 optimized to achieve the desired bandwidth for the 5G NR Band 78. In Phase 4, the Apollonian fractal structure evolves into a self-replicating network of circular elements that integrates parasitic components. This configuration enhances energy distribution and broadens the operational bandwidth, supporting efficient broadband performance. Additionally, this design antenna utilizes a microstrip feed line combined with a quarter-wavelength transformer, which optimizes the radiation pattern. These improvements are clearly demonstrated in the final design phase.

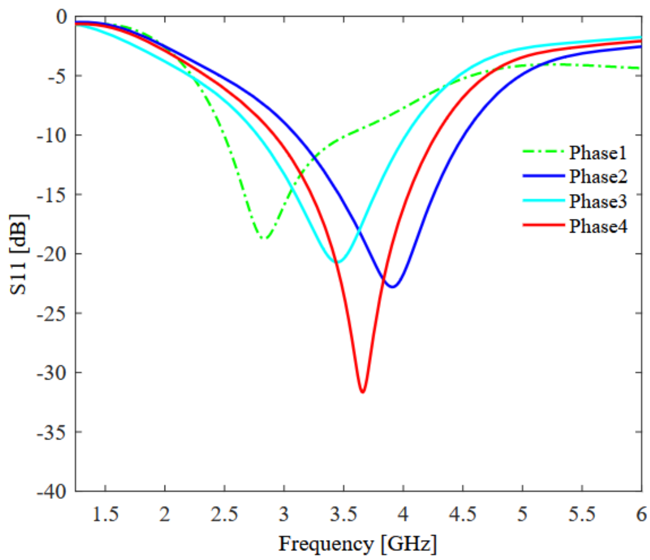

Fig. 3. S11 Parameter of the Apollony Fractal Antenna Design Evolution.

Figure 4 illustrates of current distribution across the four phases of the evolution Apollonian fractal antenna, highlighting the increasing geometric complexity and its impact on electromagnetic performance. Initially, in a single circular monopole structure, surface currents flow symmetrically and concentrate near the feed point. However, this simple configuration lacks the intricate current pathways necessary for advanced radiation characteristics. In Phase 1, the fractal begins with three mutually tangent circles that form an enclosed triangular region. This addition creates new current paths, causing the current to flow along the edges of the triangular region. Phase 2 introduces quarter-wavelength transmission lines between the circles, optimizing impedance matching and further increasing radiation efficiency, bandwidth, and reducing losses. By Phase 3, the fractal geometry becomes more intricate as the circles are slotted within the initial three. The self-similar nature of the fractal ensures that currents distribute more uniformly across the structure, leading to improved impedance matching and reduced losses. In Phase 4, the Apollonian fractal structure evolves into a self-replicating network of circular elements that incorporate parasitic elements. The self-similar nature of the fractal ensures a more uniform distribution of currents across the parasitic elements, resulting in improved impedance matching, minimizing mutual coupling (crucial for MIMO systems), and optimizing radiation patterns for broadband operation.

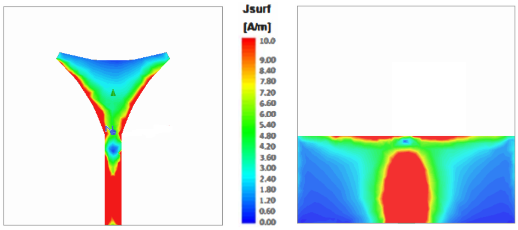

(a) Phase 1

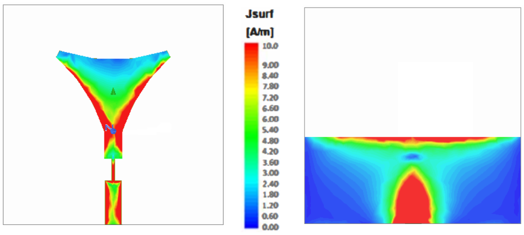

(b) Phase 2

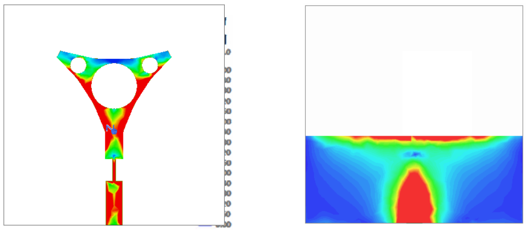

(c) Phase 3

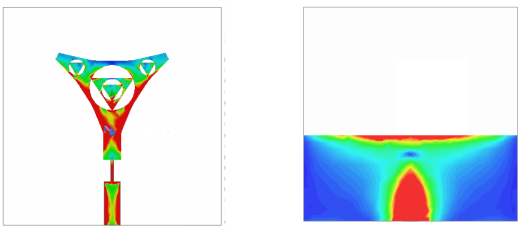

(d) Phase 4

Fig. 4. Current distribution of the Apollonian fractal antenna evolution stages.

4. Design and Fabrication of MIMO Antenna

Figure 5 illustrates the design of the Apollonian fractal MIMO antenna. The antenna features a quad-element configuration specifically designed to support NR Band 78 for 5G applications. Each antenna element incorporates an Apollonian fractal structure, a quarter-wave microstrip feedline, parasitic components, and a partial ground plane on the bottom layer. To maximize diversity and ensure optimal performance, the symmetrical elements are arranged perpendicularly with a spacing of 0.2λ. The design, based on Apollonian fractal geometry, was developed and analyzed using Computer Simulation Technology (CST), a commercial simulation software utilizing the Finite Element Method (FEM).

A physical prototype of the antenna was fabricated on a substrate with a dielectric constant (εr) of 4.3, a thickness (h) of 1.6 mm, and a loss tangent (tan δ) of 0.025. Additionally, the feedline width was set to 2.95 mm to achieve a 50 Ω characteristic impedance.

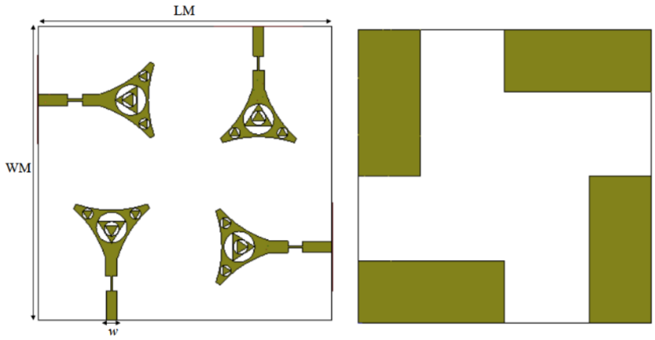

(a) Top layer (b) Back layer

Fig. 5. Geometry of the Apollony fractal MIMO antenna.

5. Characterization of MIMO Antenna

5.1. Scattering Parameter

The fabricated Apollonian-shaped fractal MIMO antenna (Fig. 6) was experimentally tested in the 5G NR78 band for MIMO applications. The scattering parameters were measured, and the signal behavior was analyzed using an R&S FSH3 Spectrum Analyzer. During the experiment, two ports of the MIMO antenna were excited, while the remaining ports were terminated with 50-ohm loads.

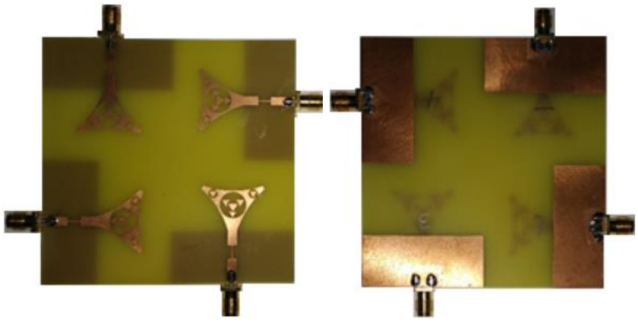

(a) Top layer (b) Back layer

Fig. 6. Fabricated prototype of the purposed MIMO antenna.

Figure 7 presents a comparison of the antenna's simulated and measured reflection coefficients. The results highlight a close agreement between the experimental data and simulations, demonstrating an impedance bandwidth of 3.3 GHz to 3.8 GHz. For the specified frequency band, the antenna exhibits a reflection coefficient smaller than -10 dB, pointing to propitious impedance adaptation qualities.

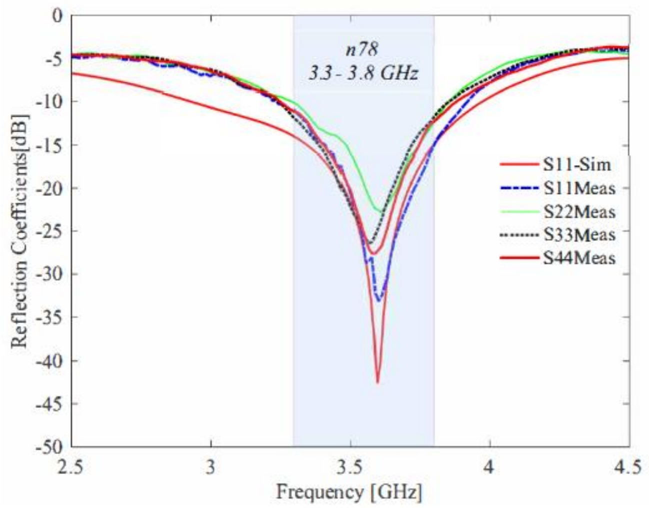

Fig. 7. Reflection coefficients of the Apollony fractal MIMO antenna

The optimal terminal configuration for the Apollonian-shaped fractal antenna was identified through initial simulations aimed at achieving high isolation and effective impedance matching. As illustrated in Fig. 8, both the experimental and simulated data indicate that the isolation between adjacent elements (S21, S41, S43) is below -20 dB, while the mutual coupling between diagonal elements (S31) remains under -25 dB throughout the operating frequency range. The isolation findings from simulation align fairly well with experimental measurements; however, the measured data shows a slight reduction in isolation, likely due to manufacturing imperfections, soldering challenges, and the use of lossy dielectric materials.

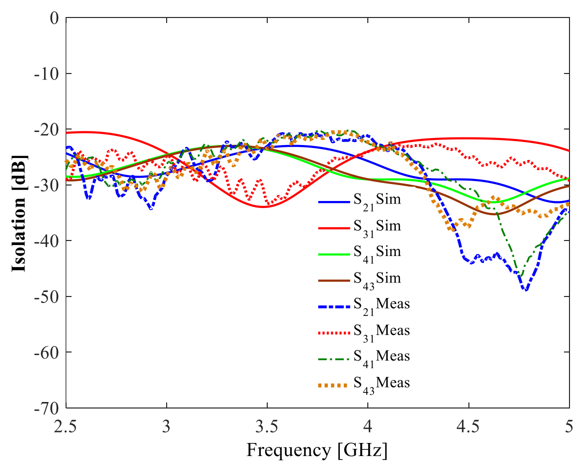

Fig. 8. Isolation Characteristics of the Apollony fractal MIMO antenna.

5.2. Envelope Correlation Coefficient

The Envelope Correlation Coefficient (ECC) quantifies the correlation between neighboring radiating antenna elements in a MIMO system [11]– [13]. Figure 9 presents experimental ECC measurements, which show good agreement with simulation results. The measured ECC values are less than 0.05 between adjacent antenna elements (ρ_{21}, ρ_{41}) and less than 0.03 between diagonal antenna elements (ρ_{31}). These low ECC values indicate that the Apollonian-shaped fractal MIMO antenna provides improved diversity performance.

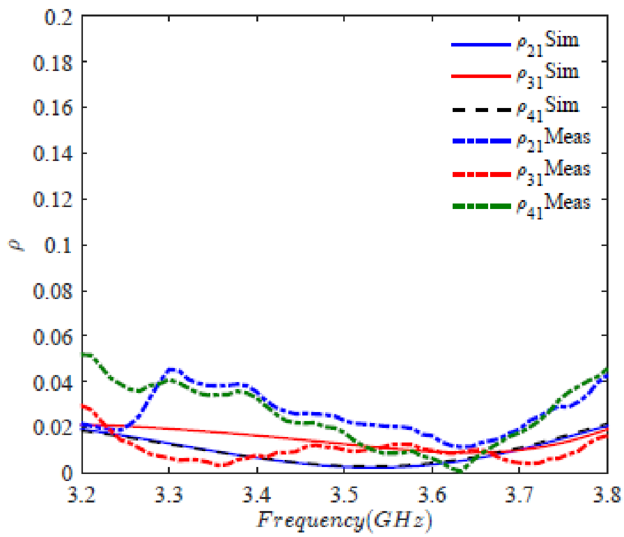

Fig. 9. Simulated and measured ECC of the Apollony fractal MIMO antenna.

5.3. Current density

The four-element Apollonian fractal antenna array is designed to achieve spatial diversity, with the elements arranged orthogonally and spaced 0.2λ apart. The symmetrical monopoles are oriented perpendicularly to enhance pattern diversity in the MIMO configuration. When antenna Element 1 is excited, the current distribution becomes strongly localized around its radiating slot, as illustrated by the driven element in Fig. 10. Notably, parasitic coupling induces current flow in Element 4 due to its orthogonal orientation, while significantly weaker currents are observed in Elements 2 and 3. This behavior highlights the array's effective decoupling, achieved through a combination of spatial separation and fractal geometry. These design features reduce mutual coupling while preserving diversity performance.

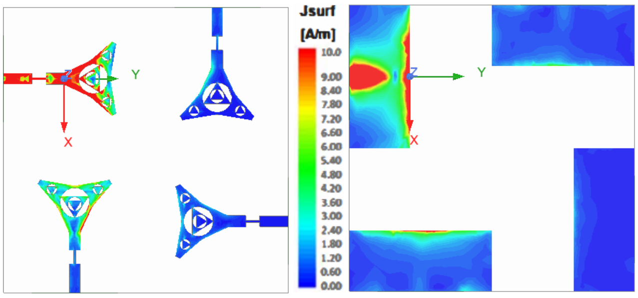

(a) Top layer (b) Back layer

Fig. 10. Current Distribution of the Apollony fractal MIMO antenna

5.4. *Gain and Efficiency of the Apollonian MIMO Antenna*

As illustrated in Fig. 11, the realized gain and radiation efficiency parameters derived from the modeling of the Apollony fractal MIMO antenna configuration are presented. The gain of the Apollony MIMO antenna retains over the working frequency from 5 to 5.5dB. In comparison, the antennas simulated radiation efficiency maintains in the operating bandwidth as a minimum value of 77%.

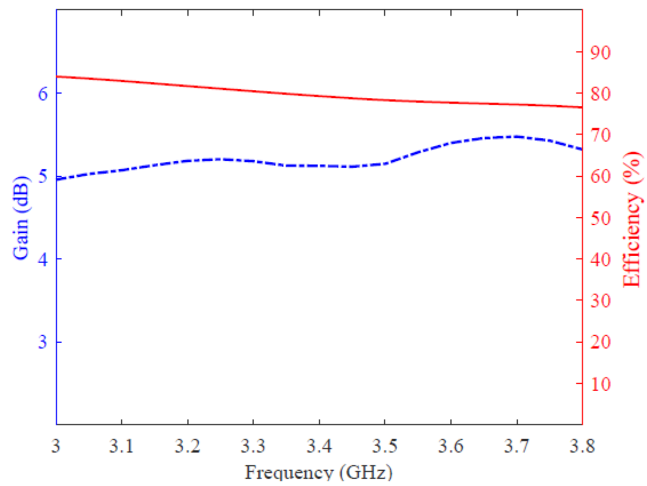

Fig. 11. Radiation Efficiency and gain of the Apollony MIMO antenna

5.5. *Radiation patterns of the Apollonian Fractal MIMO Antenna*

The radiation patterns of the electromagnetic waves emitted by the antenna in the xz- and yz-planes are presented in Fig. 12, covering the tested frequencies of 3.4 GHz, 3.6 GHz, and 3.8 GHz. Antenna elements 1 and 3 operate with vertical polarization (VP), while elements 2 and 4 operate with horizontal polarization (HP). Each element demonstrates a 5.4 dB gain, a well-defined main lobe, and a cross-polarization level suppressed below -10 dB, indicating desirable radiation characteristics and symmetrical patterns. The results confirm that the antenna's radiation patterns align well with the values obtained from CST and HFSS simulations.

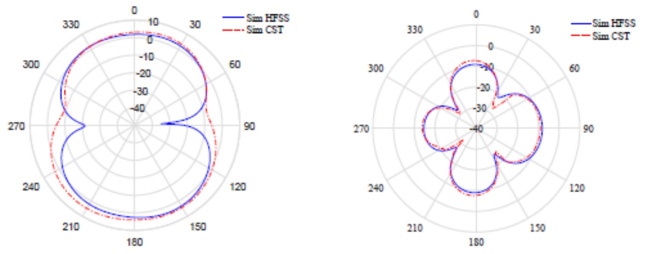

(a) xz-planes at 3.4GHz (b) yz-planes at 3.4GHz

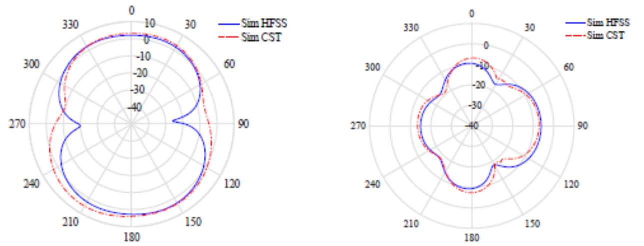

(a) xz-planes at 3.6GHz. (b) yz-planes at 3.6GHz.

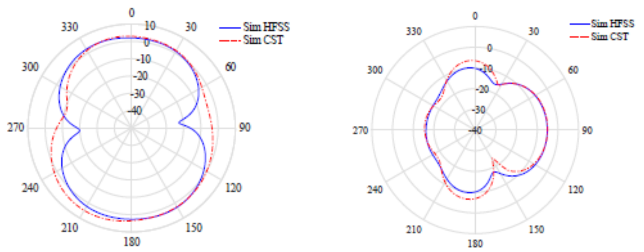

(a) xz-planes at 3.8GHz. (b) yz-planes at 3.8GHz.

Fig. 12. Radiation patterns of the Apollony fractal MIMO antenna.

5.6. *Channel capacity loss*

The CCL refers to the maximum data transmission rate at which a signal can be conveyed with minimal errors [14] - [15]. In this investigation, the CCL of the proposed antenna was analyzed using S-parameters obtained from both simulations and experimental measurements. As depicted in Fig. 13, the maximum CCL over the entire operational bandwidth remained under 0.6, demonstrating the MIMO antenna system's satisfactory diversity performance. Minor deviations between the simulated and measured CCL values can be ascribed to fabrication inaccuracies and soldering variations.

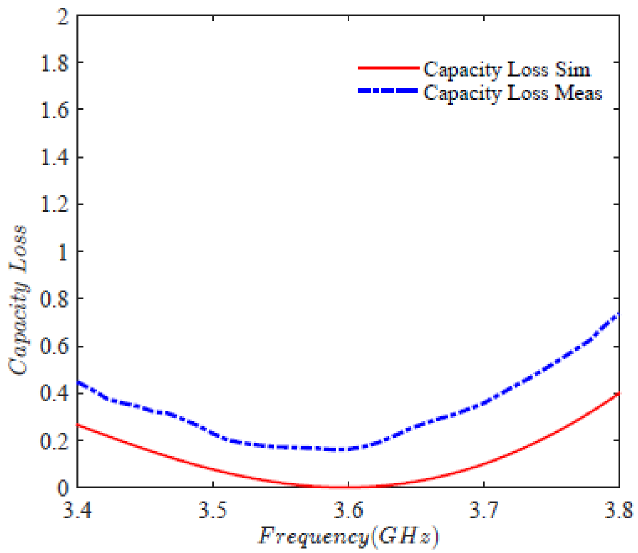

Fig. 13. Simulated and measured capacity loss of the Apollony MIMO antenna

5.7. Channel Capacity

Figure 14 illustrates the ergodic channel capacity of the proposed MIMO antenna system under fading conditions. It compares the capacity of an independent and identically distributed (i.i.d.) channel, representing an ideal uncorrelated scenario, with the simulated and measured capacities that account for realistic channel correlations. The results show a close agreement between the simulated and measured capacities, both of which approximate the capacity of the i.i.d. channel.

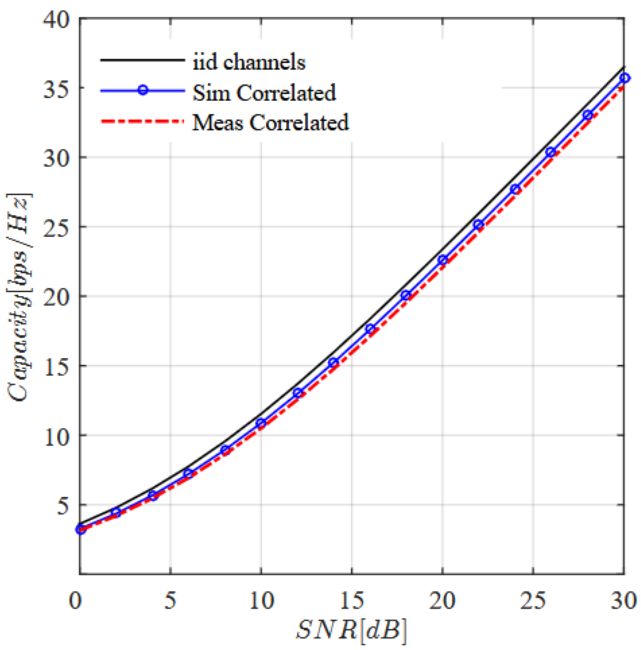

Fig. 14. Ergodic capacity of the Apollony fractal MIMO antenna

This indicates that the proposed antenna system effectively mitigates the negative effects of channel correlation. Therefore, minimizing correlation between antenna elements is crucial in MIMO systems, as lower correlation leads to higher channel capacity, allowing the system to approach the theoretical maximum achievable in an ideal uncorrelated environment.

The Apollonian MIMO antenna, when compared with other quad-element planar MIMO antennas in the literature, offers several advantages, as summarized in Table 2. These advantages include compact dimensions, excellent isolation, good gain, and low envelope correlation coefficient (ECC). The compact size of the antenna makes it highly suitable for space-constrained applications, while its high isolation reduces interference and enhances signal integrity. Furthermore, the antenna's good gain facilitates efficient signal transmission and reception, and its low ECC indicates minimal correlation between antenna elements. This results in improved diversity gain and increased channel capacity. In addition, the proposed antenna achieves a higher gain of 5.4 dB, while maintaining comparable isolation of -20 dB and a lower envelope correlation coefficient (ECC) of 0.05, compared to the other designs. The antenna also features a simpler design and easier fabrication process, making it more practical for deployment in real-world applications. Compared to previously reported designs [8], [13], [17], [18], the Apollonian MIMO antenna's compact dimensions and excellent isolation represent a significant improvement, making it a competitive and promising candidate for various high-performance MIMO system applications.

Table 2. Comparison of the Apollonian fractal MIMO antenna with previously documented antennas.

Ref.	Dim. (mm)	No. El.	Op. band (GHz)	Isol. (dB)	Gain (dB)	ECC
[8]	120x120	4	3.09 -11.36	>18	6	<0.1
[13]	82.7x82.7	4	1.68 -2.24	>13	3	<0.01
[17]	81x87	4	3.01-12.5	>20	4	<0.05
[18]	80x80	4	3.18 -11.5	>20	4	<0.15
Proposed antenna	80x80	4	3.3 -3.8	>20	5.4	<0.05

El.-Element *Isl.-Isolation* *Op.-operational*

6. Conclusion

This research aimed to examine the design and performance of a 4x4 MIMO antenna with an Apollonian fractal configuration for 5G applications. The antenna design, featuring an inter-element spacing of 0.2λ, underwent extensive modeling and analysis using the CST software platform. A prototype was constructed to allow for experimental measurement of S-parameters, yielding valuable intuitions into the diversity capabilities of the antenna design. The results demonstrate that the reflection coefficient (S11) is below -10 dB within the frequency range of 3.2 GHz to 3.8 GHz, thereby effectively covering the intended 5G operating band. The Mutual Coupling (MC) between neighboring antenna components stayed underneath -20 dB, suggesting proficient seclusion. The diversity performance, evaluated through measurements of the fabricated antenna, exhibited strong agreement with simulation results. Specifically, a correlation (ECC) below 0.05 and a capacity loss below 0.6 were achieved. The proposed antenna demonstrates favorable characteristics, including suitable bandwidth for the 5G NR Band 78, low mutual coupling, and robust diversity performance. These attributes, coupled with its compact size, position it as a promising candidate for integration into 5G portable communication devices.

References

[1] E. Dahlman, S. Parkvall, and J. Sköld, 5G Nr: The next Generation Wireless Access Technology. Amsterdam: Academic Press, 2018.

[2] H. Holma, A. Toskala, and T. Nakamura, 5G Technology: 3GPP New Radio. Hoboken, NJ: John Wiley & Sons, Inc, 2020.

[3] M. Enescu, 5G New Radio: A Beam-Based Air Interface. Hoboken, NJ, USA: Wiley, 2020.

[4] J. Malik, A. Patnaik, and M. V. Kartikeyan, Compact Antennas for High Data Rate Communication: Ultra-Wideband (UWB) and Multiple-Input-Multiple-Output (MIMO) Technology. Cham: Springer International Publishing: Imprint : Springer, 2018.

[5] R. Gurjar, D. K. Upadhyay, B. K. Kanaujia, and K. Sharma, “A novel compact self-similar fractal UWB MIMO antenna,” International Journal of RF and Microwave Computer-Aided Engineering, vol. 29, no. 3, Dec. 2018. doi:10.1002/mmce.21632

[6] A. Bhattacharya, B. Roy, S. K. Chowdhury, and A. K. Bhattacharjee, “Computational and experimental analysis of a low-profile, isolation-enhanced, band-notch UWB-MIMO antenna,” Journal of Computational Electronics, vol. 18, no. 2, pp. 680–688, Feb. 2019. doi:10.1007/s10825-019-01309-3

[7] S. Das, K. Chattopadhyay, and S. R. Bhadra Chaudhuri, “Bandwidth enhancement of a wide slot antenna using fractal geometry for UWB application with multiple notched bands,” Wireless Personal Communications, vol. 110, no. 2, pp. 677–698, Sep. 2019. doi:10.1007/s11277-019-06749-5

[8] S. Tripathi, A. Mohan, and S. Yadav, “Performance study of a fractal UWB MIMO antenna for on-body WBAN applications,” Analog Integrated Circuits and Signal Processing, vol. 95, no. 2, pp. 249–258, Feb. 2018. doi:10.1007/s10470-018-1138-0

[9] M. Mungan, “Apollonian networks: Simultaneously scale-free, Small World, euclidean, space filling, and with matching graphs,” Physical Review Letters, vol. 106, no. 2, Jan. 2011. doi:10.1103/physrevlett.106.029802

[10] C. A. Balanis, Antenna Theory Analysis and Design Constantine A. Balanis Aut. Hoboken, N.J: Wiley, 2016.

[11] S. Blanch, J. Romeu, and I. Corbella, “Exact representation of antenna system diversity performance from input parameter description,” Electronics Letters, vol. 39, no. 9, pp. 705–707, May 2003. doi:10.1049/el:20030495

[12] M. Ameen, O. Ahmad, and R. K. Chaudhary, “Single split-ring resonator loaded self-decoupled dual-polarized MIMO antenna for mid-band 5G and C-band applications,” AEU - International Journal of Electronics and Communications, vol. 124, p. 153336, Sep. 2020. doi: 10.1016/j.aeue.2020.153336

[13] L. Malviya, R. K. Panigrahi, and M. V. Kartikeyan, “MIMO antennas with diversity and mutual coupling reduction techniques: A Review,” International Journal of Microwave and Wireless Technologies, vol. 9, no. 8, pp. 1763–1780, May 2017. doi:10.1017/s1759078717000538

[14] Y. Sharma, D. Sarkar, K. Saurav, and K. V. Srivastava, “Three-element MIMO antenna system with pattern and polarization diversity for WLAN applications,” IEEE Antennas and Wireless Propagation Letters, vol. 16, pp. 1163–1166, 2017. doi:10.1109/lawp.2016.2626394

[15] W. A. E. Ali and A. A. Ibrahim, “A compact double-sided MIMO antenna with an improved isolation for UWB applications,” AEU - International Journal of Electronics and Communications, vol. 82, pp. 7–13, Dec. 2017. doi: 10.1016/j.aeue.2017.07.031

[16] L. Malviya, R. K. Panigrahi, and M. V. Kartikeyan, “A low profile planar MIMO antenna with Polarization Diversity for LTE 1800/1900 applications,” Microwave and Optical Technology Letters, vol. 59, no. 3, pp. 533–538, Jan. 2017. doi:10.1002/mop.30329

[17] K. Srivastava, A. Kumar, B. K. Kanaujia, S. Dwari, and S. Kumar, “A CPW-fed UWB MIMO antenna with integrated GSM band and dual band notches,” International Journal of RF and Microwave Computer-Aided Engineering, vol. 29, no. 1, Oct. 2018. doi:10.1002/mmce.21433

[18] M. N. Hasan, S. Chu, and S. Bashir, “A DGS monopole antenna loaded with u-shape stub for UWB MIMO applications,” Microwave and Optical Technology Letters, vol. 61, no. 9, pp. 2141–2149, May 2019. doi:10.1002/mop.31877